Detection of Energetic Particles

by

a network of HF propagation paths in Alaska.

Alfred Y. Wong

HIPAS Observatory and Dept of Physics and Astronomy, UCLA.

RADHEP-2000 , UCLA. Nov 16-18, 2000.

1. **Energetic particle causes ionization at lower heights of the atmosphere.**

2. **The more energetic the particle the lower it reaches down in the atmosphere.**

3. **HF horizontal propagation paths are sensitive to plasma density in the atmosphere.**

4. **Phase sensitive detection allows lower limit of detection of charge densities. Phase-loop method is sensitive to 0.1 degree.**

5. **Calibration by laser produced plasmas. Laser on dust target.**

Three concepts:

1. All Alaska monitoring using cell phone base stations.

2. Laser focused by large (2.7 M) rotating mercury mirror.

Laser-dust interactions produce plasmas in the lower ionosphere for calibration and to act Artificial Ionospheric Mirror.

3. Platforms in the Troposphere and Stratosphere made possible by new types of ion engines.

$$\Delta\phi = \int_0^L \left(k_{vacuum} - k_{plasma} \right) dx,$$

Assuming constant n_e through length L, we have:

$$\Delta\phi = \frac{\omega}{c}\left[1 - \left(1 - \frac{\omega_{pe}^2}{\omega^2} \right)^{1/2} \right] L$$

$$k_{vacuum} = \frac{\omega}{c} \quad \text{and} \quad k_{plasma} = \frac{\left(\omega^2 - \omega_{pe}^2 \right)^{1/2}}{c}$$

$$\omega_{pe} = \left(\frac{4\pi n_e e^2}{m_e} \right)^{1/2} = 5.64 x 10^4 n_e^{1/2} \quad \text{(rad/s)}$$

Case 1: $\Delta\phi = 0.02$ rad (~ 1°)

A. for frequency = 4.95 MHz ($\omega \sim 3.1 \times 10^7$ rad/sec)

L (km)	ω_{pe} (rad/sec)	N_e (cm^{-3})
1	6.11×10^5	117.3
10	1.93×10^5	11.73
100	0.61×10^5	1.173

Case 1: $\Delta\phi = 0.02$ rad (~ 1°)

B. for frequency = 2.85 MHz ($\omega \sim 1.79 \times 10^7$ rad/sec)

L (km)	ω_{pe} (rad/sec)	N_e (cm^{-3})
1	4.64×10^5	67.5
10	1.47×10^5	6.75
100	0.46×10^5	0.676

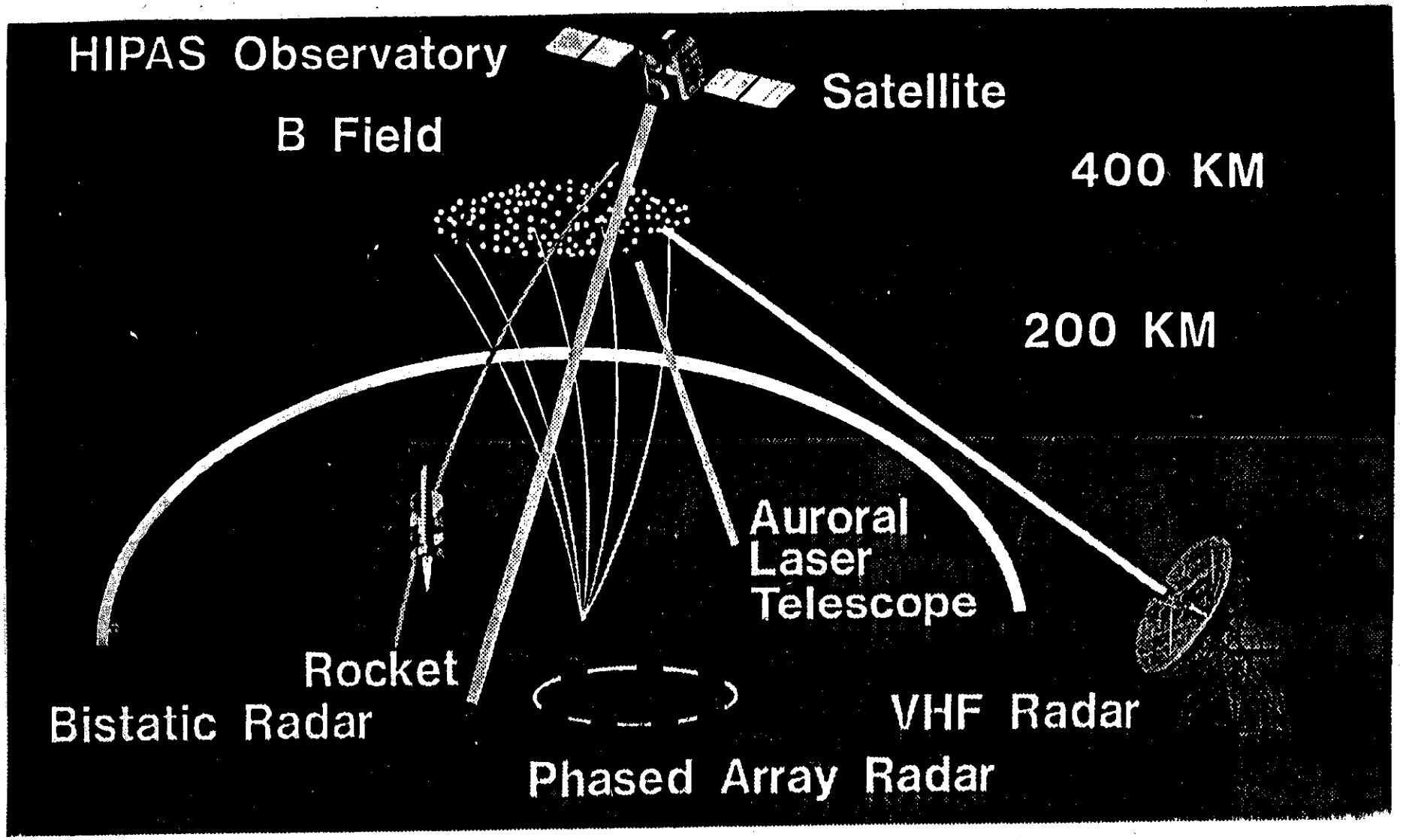
HIPAS Observatory
B Field
Satellite
400 KM
200 KM
Auroral
Laser
Telescope
Rocket
Bistatic Radar
VHF Radar
Phased Array Radar

Figure 9a

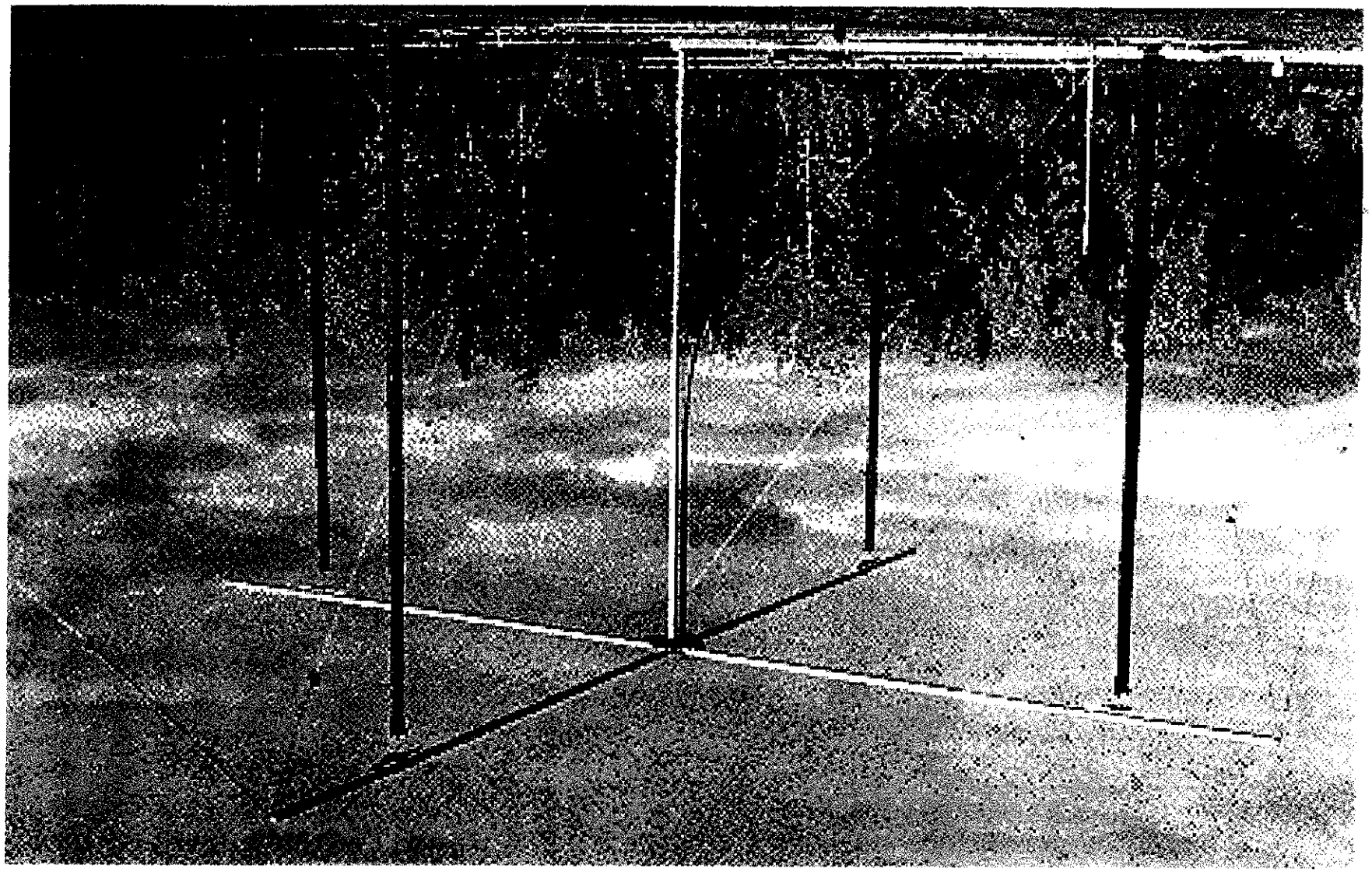

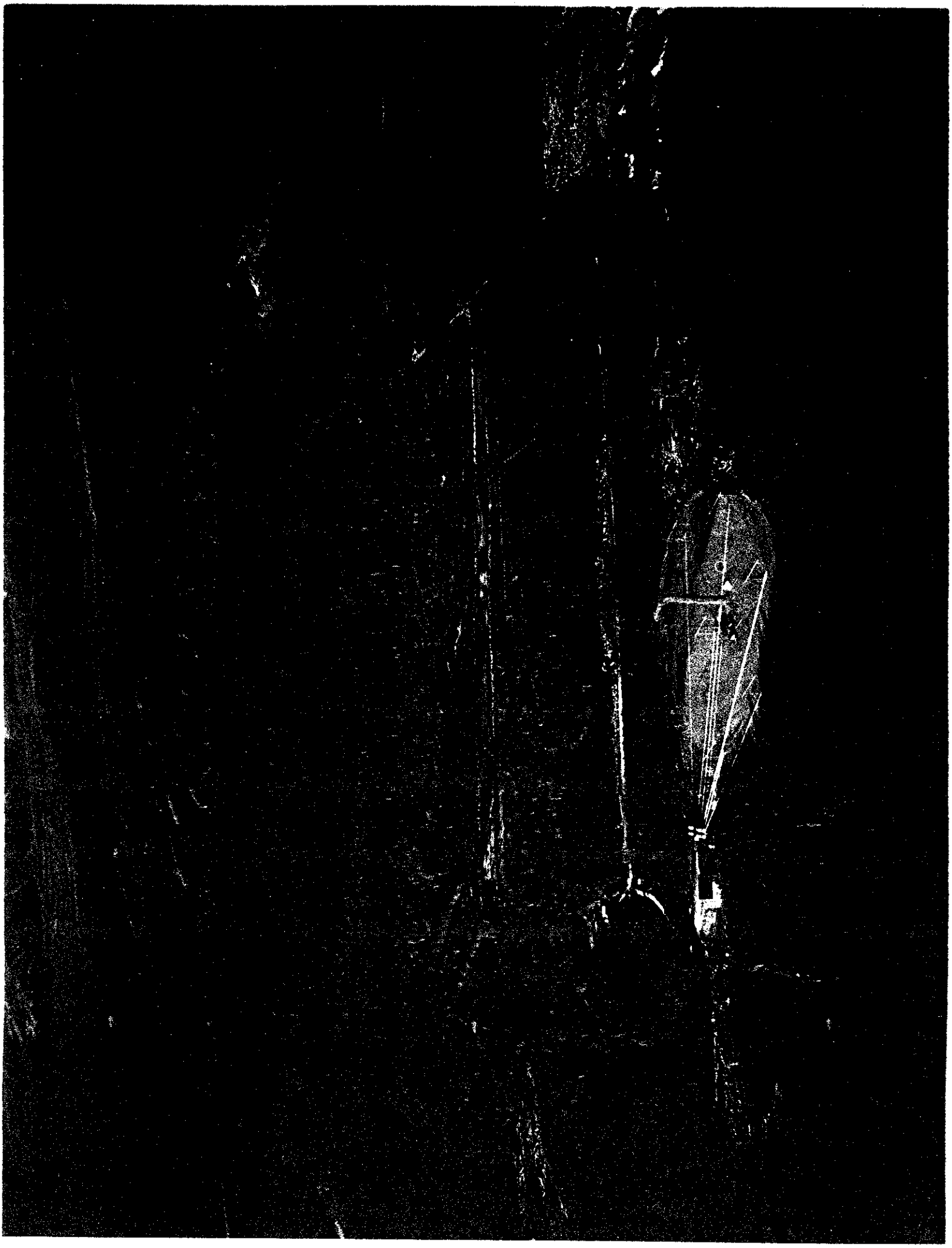

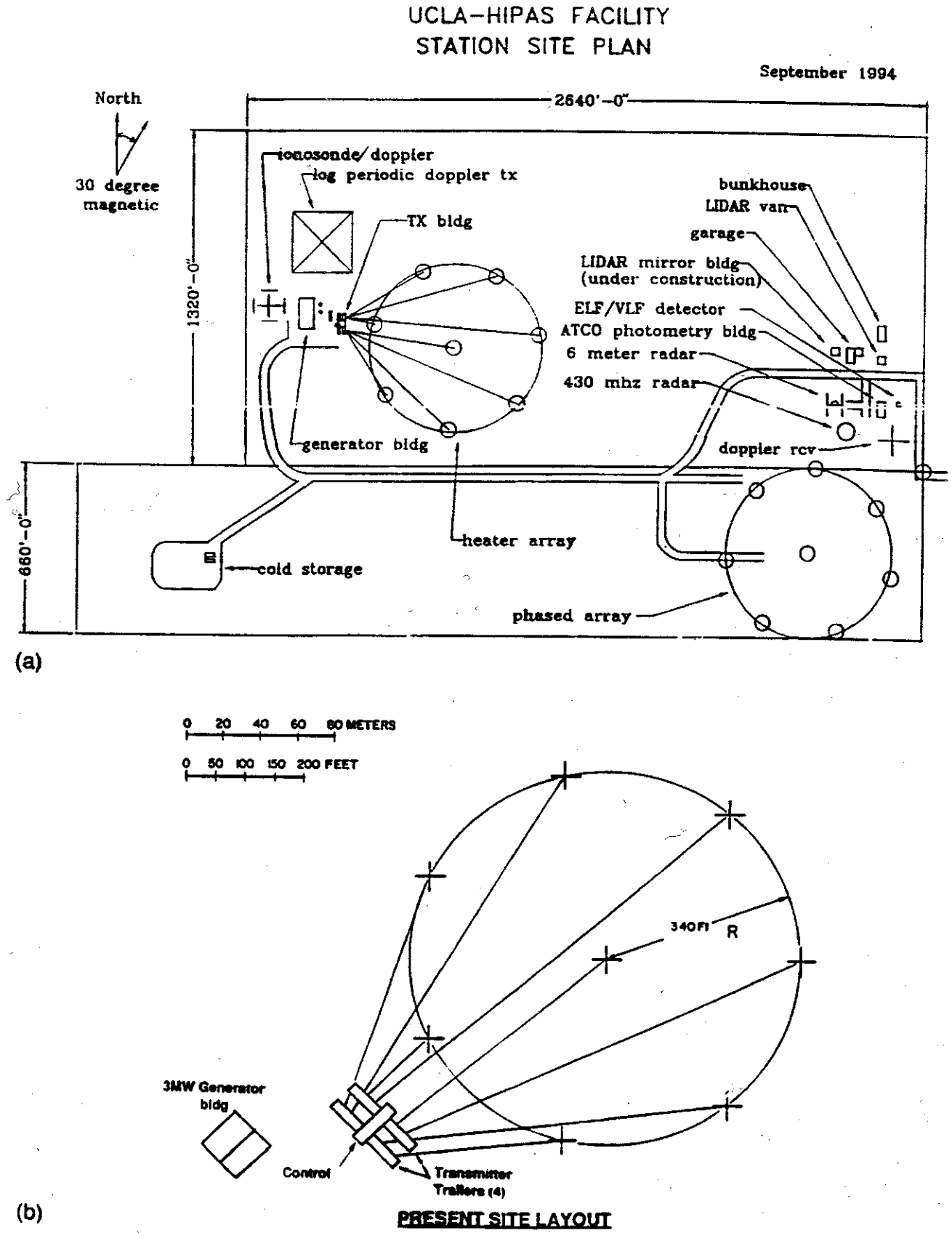

FIGURE 3.8. (a) UCLA–HIPAS facility station site plan, showing on-site diagnostics and the high-power heater. (b) Schematic of the present HIPAS ionospheric radio-frequency heater showing the eight antennas, each connected to a transmitter, with a total output power of 1.25 MW.

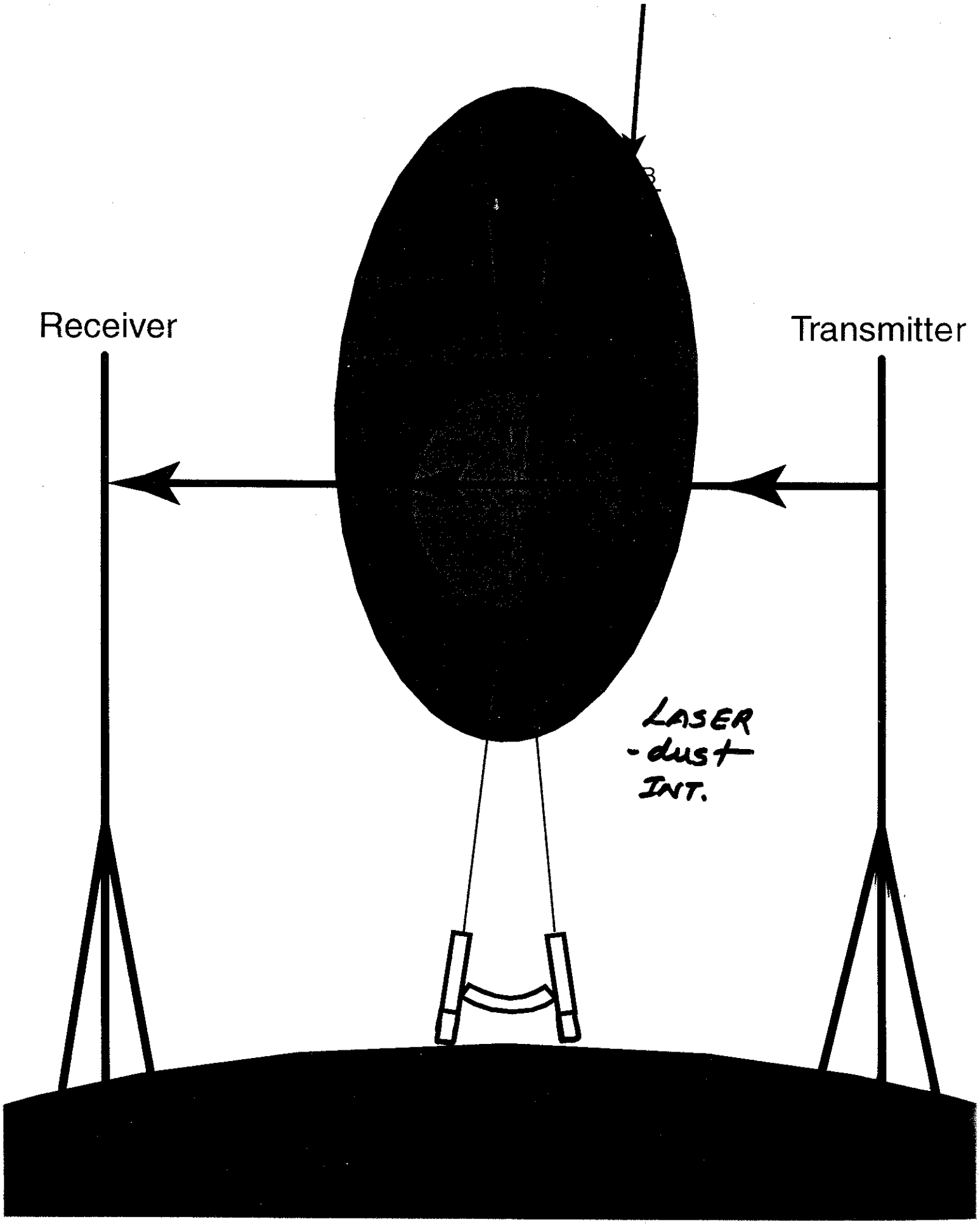
Receiver
Transmitter
LASER
- dust
INT.

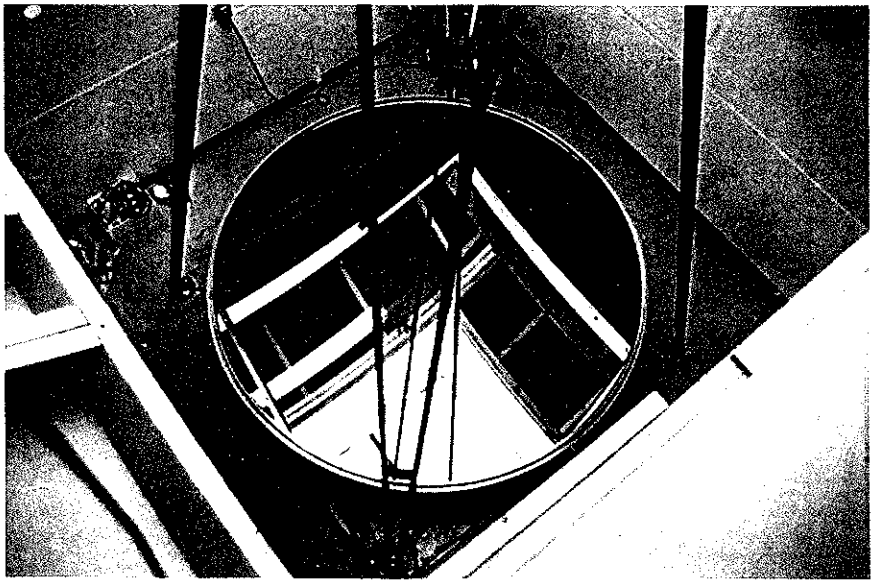

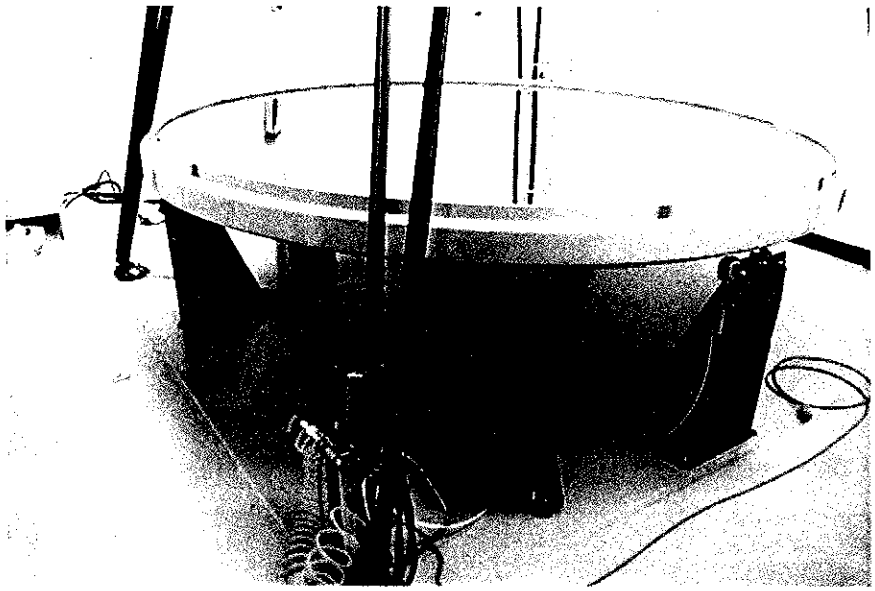
2.7 M
0
100 in.

Why HF paths ? Easy to see phase shift and detectors are readily available.

Phase shift is proportional to Line Density and inversely

proportional to (probing frequency)^2

Phase loop stability technique allows us to see

$$N \times L = 10^5 \text{ to } 10^6 \text{ cm}^{-2}$$

Estimate by Wick et al. $dE/dx = 10^5$ Tev/atm

Yields $N \times L = 3 \times 10^5$ to 3×10^6 cm^{-2}

The effects should be observable if

the attachment time is > 0.2 us

Alaska has clean dry air and the electron attachment time in the presence of ionization radiation can be $>$ 1 us.

Ideal Homogeneous Atmosphere

FROM R. WUERKER, UCLA

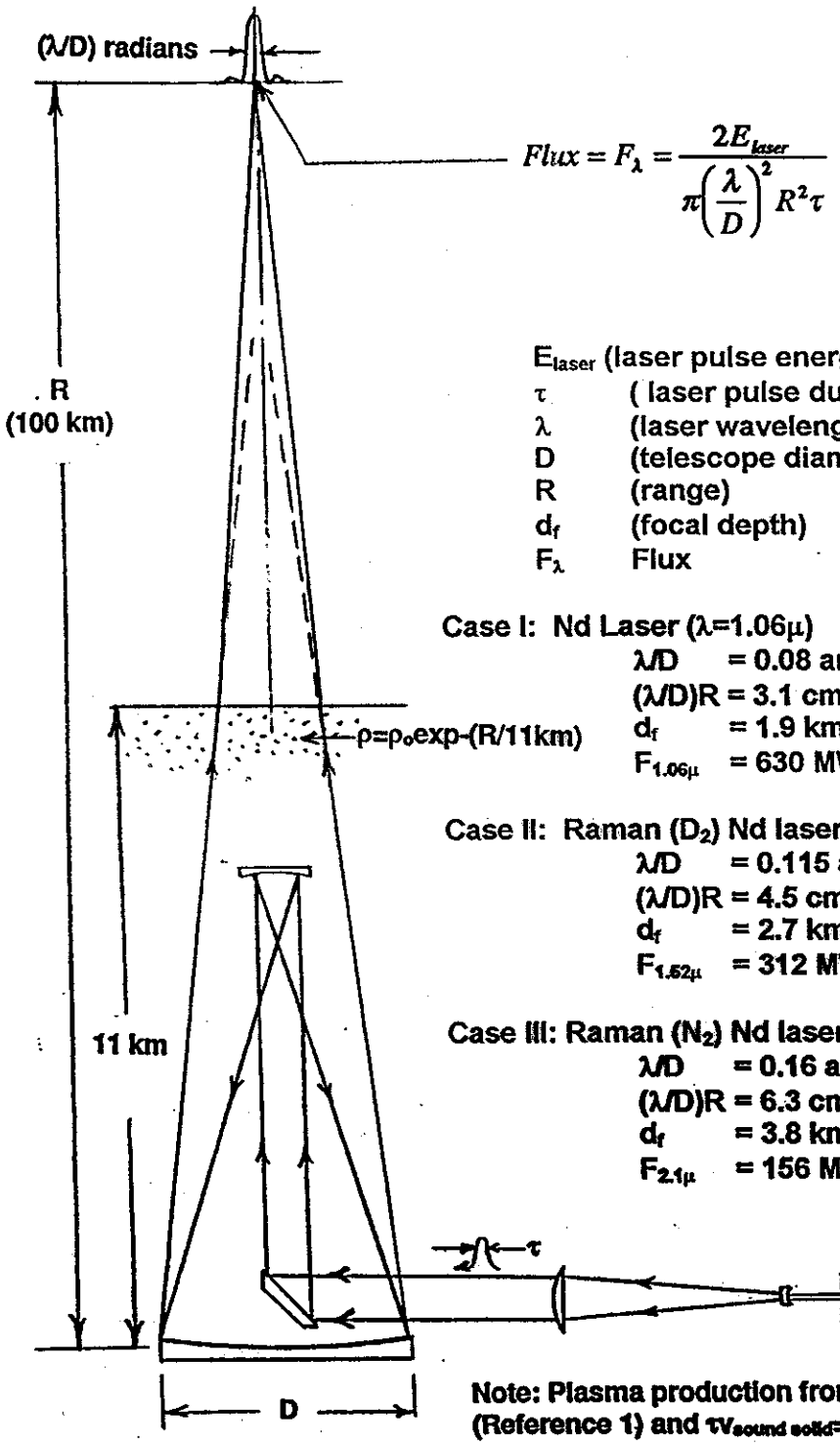

E_{laser}	(laser pulse energy)	= 10 Joules
τ	(laser pulse duration)	= 1 nsec
λ	(laser wavelength)	
D	(telescope diameter)	= 2.7 m
R	(range)	= 80 km
d_f	(focal depth)	= $2\lambda (R/D)^2$
F_λ	Flux	$\cong 2E_{laser}/\pi\tau(\lambda R/D)^2$

Case I: Nd Laser (λ=1.06μ)

- λ/D = 0.08 arc seconds
- $(\lambda/D)R$ = 3.1 cm
- d_f = 1.9 km
- $F_{1.06\mu}$ = 630 MW/cm^2

Case II: Raman (D_2) Nd laser (λ=1.52μ)

- λ/D = 0.115 arc sec
- $(\lambda/D)R$ = 4.5 cm
- d_f = 2.7 km
- $F_{1.52\mu}$ = 312 MW/cm^2

Case III: Raman (N_2) Nd laser (λ=2.1μ)

- λ/D = 0.16 arc sec
- $(\lambda/D)R$ = 6.3 cm
- d_f = 3.8 km
- $F_{2.1\mu}$ = 156 MW/cm^2

Note: Plasma production from solid targets starts at 10^8W/cm^2 (Reference 1) and $\tau v_{sound\ solid}$= (1ns)(5km/s) = 5 μ particle diameter.

Figure 1 Proposed Gregorian arrangement for focusing laser radiation to high altitudes through an ideal homogenous atmosphere. Fluxes for 10 J/pulse - 1 nanosecond duration lasers focused to 80 km are included.

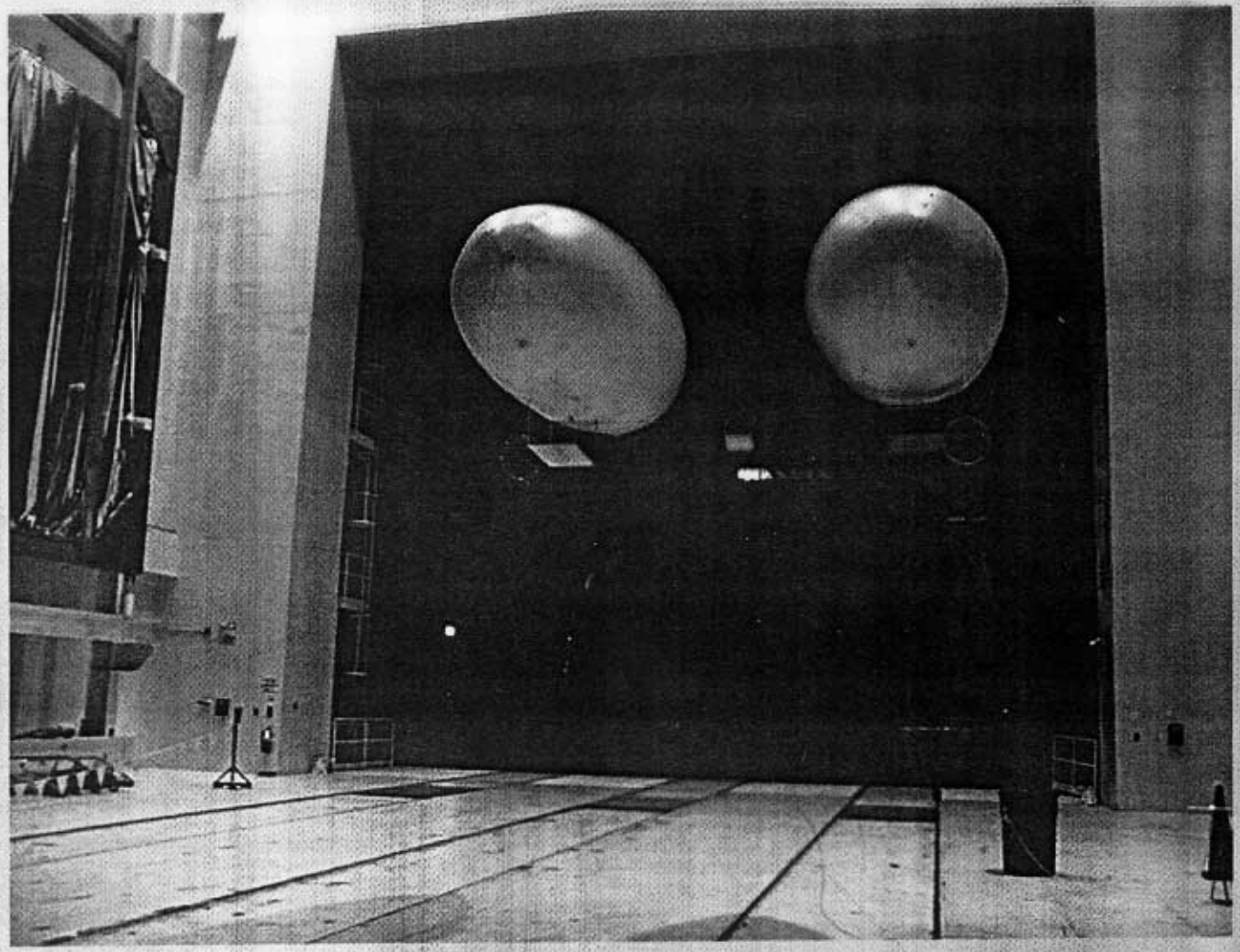

Fig 8c Platform driven by NIPE ion engines at NASA Plum Brook test Facility.

HEWLETT PACKARD

PACKARD PACKARD PACKARD PACKARD

Electrons N

$$\frac{dN}{dt} = q_i + \nu_{im} N - \nu_a N + \nu_d N^- - \alpha N (N + N^-)$$

$$\frac{dN^-}{dt} = \nu_a N - \nu_d N^- - \alpha N^- (N + N^-)$$

negative ions

$$\nu_a \cong k_1 N_{O_2} N_{O_2}$$ TRIPLE COLLISIONS

GOREVICH PHELPS $k_1 = 1.4 \times 10^{-29} \exp\left(-\frac{600}{T_e}\right) cm^6/s$

$$\nu_d \cong \nu_{ph} + R_6 N_{O_2'} + k_7 N_O + k_8 N_N$$

COLLISIONS WITH O_2^* — WITH O — WITH N

$$N \cong N^+ \frac{\nu_d}{\nu_a + \nu_d}$$ $\nu_a, \nu_d \gg \alpha N$

GCI NETWORK

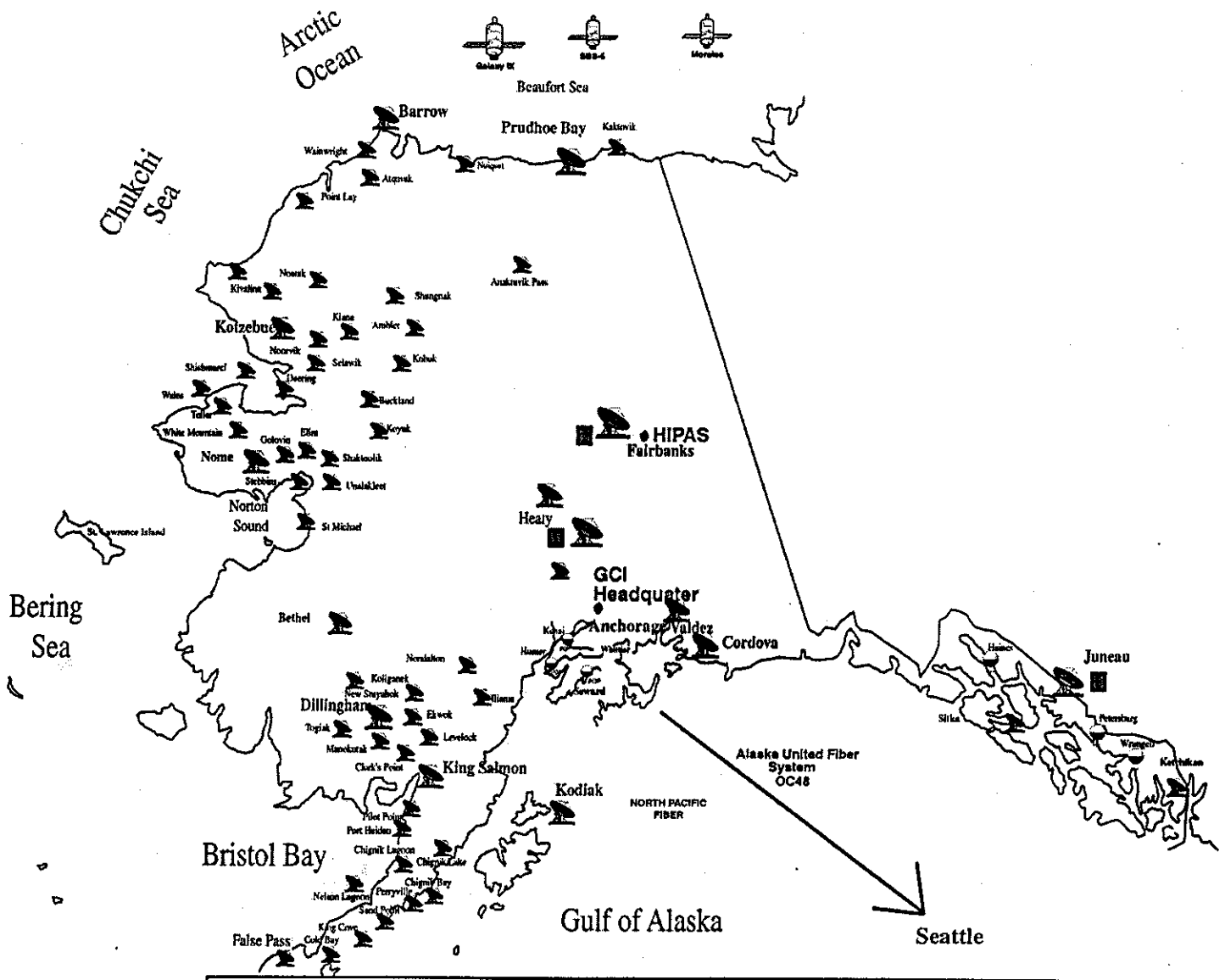

Figure 1 Location of GCI communications network sites

the appearance of negative ions, play an essential role. The ionization balance equations for the concentrations N of the electrons and N^- of the negative ions then take the form

$$\begin{aligned} \frac{dN}{dt} &= q_i + \nu_{ion}N - \nu_a N + \nu_d N^- - \alpha N(N + N^-), \\ \frac{dN^-}{dt} &= \nu_a N - \nu_d N^- - \alpha_i N^-(N + N^-). \end{aligned} \tag{2.251}$$

Here, as usual, q_i is the total intensity of the ionization produced by the external source and ν_{ion} is the frequency of the molecule ionization by the fast electrons [Eqs. (2.177), (2.178)]. We note that the exponential in Equation (2.177) contains a large quantity, so that the dependence of ν_{ion} on E_0, ω, and N_m is determined in the main by the exponential term.

Next, ν_a is the frequency of electron attachment to the molecules. Under the conditions of the lower ionosphere, an important role is played by the attachment of electrons to oxygen molecules in triple collisions, and also by dissociative attachment to the ozone and oxygen molecules

$$\nu_a = (k_1 N_{O_2} + k_2 N_{N_2})N_{O_2} + k_3 N_{O_3} + k_a N_{O_2} \tag{2.251a}$$

Here k_1 and k_2 are the attachment coefficients for triple collisions. According to Phelps (1969),

$$k_1 = 1.4 \cdot 10^{-29} \exp\left(-\frac{600}{T_e}\right) \text{cm}^6/\text{s}, \qquad k_2 = 1.0 \cdot 10^{-31}\ \text{cm}^6/\text{s} \tag{2.251b}$$

The electron temperature is expressed here in K. The coefficient to ozone is $k_3 \simeq (1\text{–}10) \cdot 10^{-12}\ \text{cm}^3/\text{s}$. The coefficient of dissociative attachment to oxygen k_a is given by Equation (2.177a) and (2.178a).

Next, ν_d is the electron detachment frequency. Important processes in the ionosphere are photodetachment, detachment in collisions with molecules, and associative detachment:

$$\nu_d = \nu_{ph} + (k_4 N_{O_2} + k_5 N_{N_2} + k_6 N'_{O_2}) + (k_7 N_O + k_8 N_N). \tag{2.251c}$$

Here ν_{ph} is the photodetachment frequency; under conditions of the daytime ionosphere, $\nu_{ph} \simeq 0.44\ \text{s}^{-1}$ (Whitten and Poppoff, 1965). The coefficients k_4 and k_5 for detachment in collisions with oxygen and nitrogen molecules, respectively, at lower-ionosphere temperatures $T \sim 200\text{–}300$ K, are small: $k_4 \sim 10^{-22}\text{–}10^{-19}\ \text{cm}^3/\text{s}$ and $k_5 \sim 10^{-23}\text{–}10^{-20}\ \text{cm}^3/\text{s}$.

More significant here is apparently the detachment in collisions with excited oxygen, with $k_6 \approx 2 \cdot 10^{-10}$ cm^3/s (N'_{O_2} is the concentration of the excited $O_2(^1\Delta_g)$ molecules). The coefficients $k_7 = 2.5 \cdot 10^{-10}$ cm^3/s and $k_8 = 3 \cdot 10^{-10}$ cm^3/s describe associative detachment in collisions with oxygen and nitrogen atoms ($O_2^- + O \rightarrow O_3 + e$, $N + O_2^- \rightarrow NO_2 + e$). We note that we consider here detachment only for the O_2^- ions. The O^- ions vanish mainly through processes of associative detachment (Phelps, 1969).

Finally, α is the dissociative recombination coefficients:

$$\alpha = \alpha_1 n_{NO^+} + \alpha_2 n_{O_2^+} + \alpha_3 n_c. \tag{2.251d}$$

In contrast to Equation (2.223), we took into account here also dissociative recombination of heavy ion clusters $\alpha_3 n_c$, with a coefficient $\alpha_3 \sim 10^{-5}$ cm^3/s and a relative cluster concentration $n_c = N_c^+/(N^- + N)$; it rises abruptly in the region of the D layer, at $z \leq 80$ km, where the ion clusters frequently predominate (Goldberg and Aikin, 1971; Bauer, 1973; Danilov and Simonov, 1975). The recombination coefficient of the positive and negative ions is $\alpha_i \sim 10^{-7}$ cm^3/s (Biondi, 1970; Bauer, 1973).

We emphasize that the complete system of balance equations must include the equations of ion kinetics, of the type considered in Section 2.5.1. We are forced here to confine ourselves to the approximate system of Equations (2.251), since the exact composition of the negative and positive ions in the D region is still not sufficiently well known, nor are the coefficients of the corresponding ionic reactions.

We proceed to the analysis of the stationary solution of Equations (2.251). From the second equation of Equation (2.251) it follows that

$$N^- = N\nu_a/[\nu_d + \alpha_i(N + N^-)].$$

Using the quasineutrality condition $N + N^- = N^+$, we express the concentrations of the electrons and of the negative ions in terms of the concentration of the positive ions N^+

$$N = N^+ \frac{\nu_d + \alpha_i N^+}{\nu_a + \nu_d + \alpha_i N^+}, \quad N^- = N^+ \frac{\nu_a}{\nu_a + \nu_d + \alpha_i N^+}. \tag{2.251e}$$

Substituting these expressions in the first equation of Equation (2.251), we have for N^+ the cubic equation

$$q_i(\nu_a + \nu_d + \alpha_i N^+) + \nu_{ion} N^+(\nu_d + \alpha_i N^+) - N^{+2}(\alpha_i \nu_a + \alpha \nu_d + \alpha \alpha_i N^+) = 0.$$

N.Y. Times
Nov 21 '95

Spun Liquid Mercury Metal Is Eye of a New Generation of Telescopes

Mercury rivals the best glass mirrors in accuracy of images.

By MALCOLM W. BROWNE

Since Sir Isaac Newton invented the reflecting telescope three centuries ago, astronomical observatories have been largely dependent on huge and increasingly costly light-collecting mirrors made of aluminum-coated glass. But a new generation of mirrors based on silvery liquid mercury promises to drastically reduce the cost of cutting-edge astronomy.

The new mirrors are little more than rotating dishes containing small quantities of liquid mercury metal. As the mirror dish at the base of a telescope rotates, centrifugal force counters the force of gravity on the heavy fluid, pushing some of the mercury outward and upward toward the edge, curving its shiny surface into a perfect paraboloid. By adjusting the speed of rotation, and hence the curvature of the mercury's surface, the focal length of the mirror can be adjusted.

New telescopes based on liquid-mercury mirrors must look almost straight up, a limitation for an astronomical observatory. But for many purposes, including astronomical scanning, searching for space debris and probing the chemistry of the Earth's atmosphere, a vertical view is adequate.

Users of the new mercury telescopes describe the quality of their reflected images as better than those of most solid glass mirrors.

"We are getting image quality from mercury mirrors comparable to that of the glass mirror in the Hubble Space Telescope," said Dr. Ermanno F. Borra of the Université Laval in Quebec, a leading innovator in the development of spinning liquid mirrors. Best of all, a telescope with a liquid-mercury mirror costs less than one-hundredth as much as a telescope with a conventional glass mirror, he said.

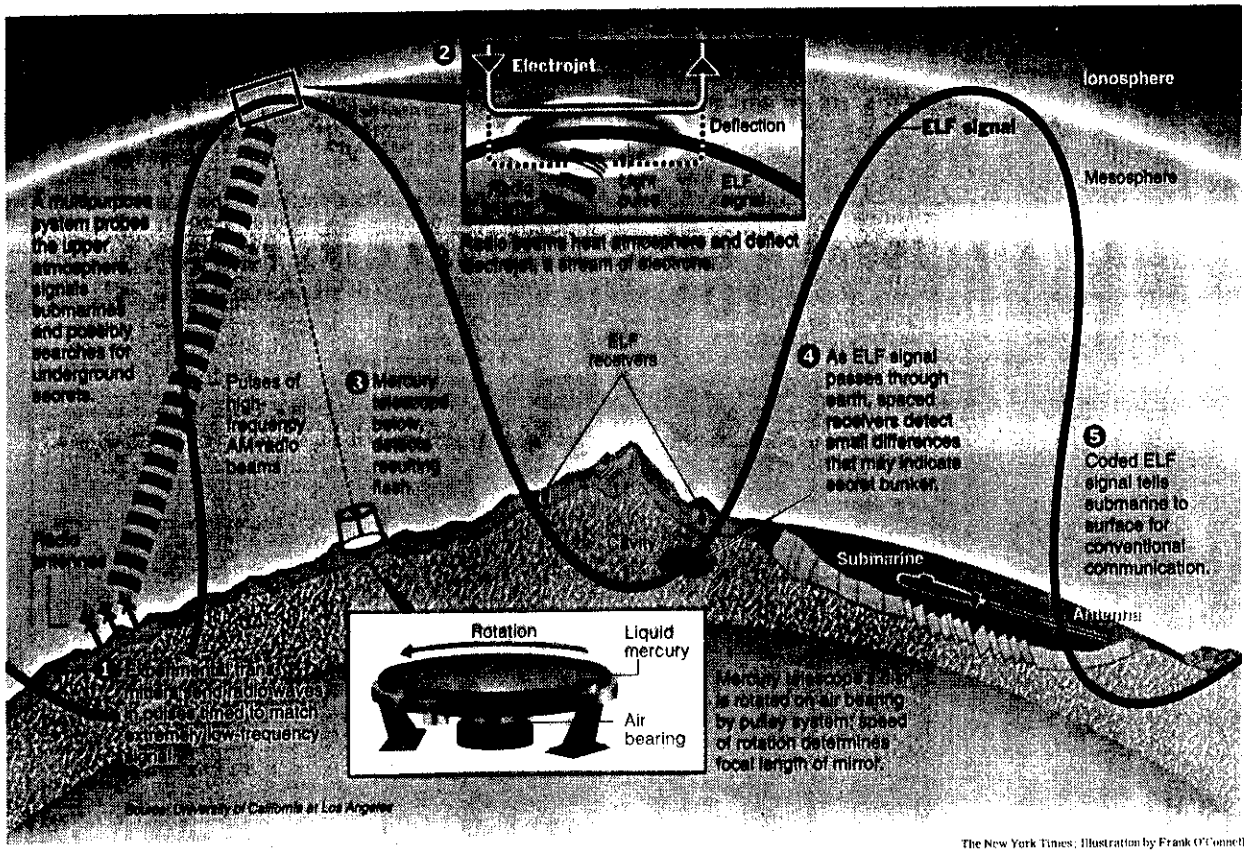

The New York Times; Illustration by Frank O'Connell

In September, the University of California at Los Angeles began operating a 2.6-meter (104-inch) mercury mirror 100 miles below the Arctic Circle 30 miles east of Fairbanks, Alaska. The telescope, the 20th largest in the world, is dedicated to studying the aurora borealis and the ionosphere, the region of the upper atmosphere where the aurora occurs. The telescope, say its builders, cost only $50,000, a small fraction of the cost of a telescope with a glass mirror of the same size.

The telescope is partly financed by the military because experiments with it may lead to new techniques for signaling submarines and probing battlefields for secret tunnels and bunkers. Users of the telescope will study the interaction of intense pulses of radio beams with the ionosphere, which then broadcasts a signal that can be received in the deep ocean. (Page B8.)

Dr. Ralph Wuerker, a U.C.L.A. development engineer, said that the instrument will spend the forthcoming winter studying ionized nitrogen in the atmosphere about 60 miles high, where solar radiation rips away some electrons from the atoms making up gases, leaving them in an electrically charged state. A laser mounted near the telescope fires brief pulses of light upward, tuned to excite the ionized gas to emit a pulse of light of its own. This return pulse is then collected by the mercury-mirror telescope, and its light is analyzed in terms of spectral composition.

Several other mercury-mirror telescopes are in operation.

At Sunspot, N.M., the National Aeronautics and Space Administration has completed a three-meter-diameter (118-inch) mercury-mirror telescope designed to collect images of space debris that might hit manned spacecraft with catastrophic results. The telescope can detect orbiting objects as small as one-half inch across as they pass overhead. NASA plans to build a similar telescope at the Equator to hasten the agency's tally of dangerous space debris.

For three years, the University of Western Ontario at London, Ontario, has operated a 2.7-meter (106-inch) mercury mirror in conjunction with an upward-pointing laser for atmospheric studies, which include the detection of changes in the protective ozone layer.

At Dr. Borra's laboratory, a 3.6-meter (142-inch) liquid mirror is under development, and Dr. Borra is collaborating with Dr. Paul Hickson of the University of British Columbia at Vancouver in the building of a gigantic five-meter mercury-mirror instrument. This telescope will have the same light-collecting power as the great 200-inch telescope at Mount Palomar, Calif., which is the third largest in the world. (Russia has a six-meter, or 236-inch, telescope; the Keck Telescope in Hawaii, 10 meters, or 393 inches, in diameter, is the world's largest.)

Mercury mirrors are so accurate, Dr. Borra said, that one of them, a 59-inch reflector built in Belgium, is used as a reference standard for testing conventional glass telescope mirrors being sent into space by the European Space Agency.

The idea of using a liquid mirror in an astronomical telescope is not new. Isaac Newton himself is believed to have thought of it.

In 1908, Dr. Robert W. Wood of Johns Hopkins University spent his summer vacation on Long Island, building a primitive observatory with a spinning liquid mercury mirror. The mirror, a dish 20 inches in diameter, was mounted on a bearing attached to a sturdy concrete foundation at the bottom of a deep pit. The mirror was turned by a pulley connected to an electric motor. By adjusting the motor's speed he could change the curvature of the mercury

Continued on Page B8